

UC Davis

UC Davis Previously Published Works

Title

Shoot dimorphism enables Sequoia sempervirens to separate requirements for foliar water uptake and photosynthesis

Permalink

<https://escholarship.org/uc/item/9jc868nk>

Journal

American Journal of Botany, 109(4)

ISSN

0002-9122

Authors

Chin, Alana RO
Guzmán-Delgado, Paula
Sillett, Stephen C
et al.

Publication Date

2022-04-01


DOI

10.1002/ajb2.1841

Peer reviewed

RESEARCH ARTICLE

Shoot dimorphism enables *Sequoia sempervirens* to separate requirements for foliar water uptake and photosynthesis

Alana R. O. Chin¹  | Paula Guzmán-Delgado¹ | Stephen C. Sillett² |
 Jessica Orozco¹ | Russell D. Kramer³ | Lucy P. Kerhoulas² | Zane J. Moore¹ |
 Marty Reed⁴ | Maciej A. Zwieniecki¹

¹Plant Sciences Department, University of California Davis Davis, CA 95616, USA

²Department of Forestry and Wildland Resources, Humboldt State University, Arcata, CA 95521, USA

³Dipper and Spruce LLC, White Salmon, WA 98672, USA

⁴Department of Biological Sciences, Humboldt State University, Arcata, CA 95521, USA

Correspondence

Alana R. O. Chin, D-USYS, ETH, Zürich 8092, Switzerland.

E-mail: alanaroseo@gmail.com

Present address

Alana R. O. Chin, D-USYS, ETH, Zürich 8092, Switzerland.

Abstract

Premise: Trees in wet forests often have features that prevent water films from covering stomata and inhibiting gas exchange, while many trees in drier environments use foliar water uptake to reduce water stress. In forests with both wet and dry seasons, evergreen trees would benefit from producing leaves capable of balancing rainy-season photosynthesis with summertime water absorption.

Methods: Using samples collected from across the vertical gradient in tall redwood (*Sequoia sempervirens*) crowns, we estimated tree-level foliar water uptake and employed physics-based causative modeling to identify key functional traits that determine uptake potential by setting hydraulic resistance.

Results: We showed that *Sequoia* has two functionally distinct shoot morphotypes. While most shoots specialize in photosynthesis, the axial shoot type is capable of much greater foliar water uptake, and its within-crown distribution varies with latitude. A suite of leaf surface traits cause hydraulic resistance, leading to variation in uptake capacity among samples.

Conclusions: Shoot dimorphism gives tall *Sequoia* trees the capacity to absorb up to 48 kg H₂O h⁻¹ during the first hour of leaf wetting, ameliorating water stress while presumably maintaining high photosynthetic capacity year round. Geographic variation in shoot dimorphism suggests that plasticity in shoot-type distribution and leaf surface traits helps *Sequoia* maintain a dominant presence in both wet and dry forests.

KEYWORDS

Cupressaceae, foliar water uptake, heteroblasty, hydraulic resistance, redwood, *Sequoia*, structural equation model, traits

Trees face trade-offs between foliar uptake and photosynthesis when leaves are wet (Smith and McClean, 1989; Ishibashi and Terashima, 1995; Dawson and Goldsmith, 2018). Water absorbed across leaf surfaces allows woody plants to avoid or recover from drought-induced hydraulic damage, maintain higher photosynthetic rates, relieve low xylem water potentials (Ψ), and initiate turgor-driven diameter growth (Breshears et al., 2008; Eller et al., 2013; Emery, 2016; Steppe et al., 2018). Trees, which

may be reliant on foliar uptake to cope with height-associated water stress, may have leaf-surface traits more associated with water absorption than small-statured plants in similar environments (Neinhuis and Barthlott, 1997; Schreel and Steppe, 2020). However, if leaf stomata are covered by films of water, photosynthesis can be suppressed (Smith and McClean, 1989; Ishibashi and Terashima, 1995; Hanba et al., 2004; Gerlein-Safdi et al., 2018; Berry and Goldsmith, 2020). Ability to absorb water through leaves is

This is an open access article under the terms of the Creative Commons Attribution-NonCommercial-NoDerivs License, which permits use and distribution in any medium, provided the original work is properly cited, the use is non-commercial and no modifications or adaptations are made.

© 2022 The Authors. *American Journal of Botany* published by Wiley Periodicals LLC on behalf of Botanical Society of America.

widespread, but its capacity may be highly variable within and among taxa and environments (Gotsch et al., 2015; Dawson and Goldsmith, 2018; Binks et al., 2019). In seasonally dry forests, foliar uptake can be a key component of tree drought survival (Yates and Hutley, 1995; Schreel et al., 2019), whereas trees in perpetually wet forests may have evolved adaptations to avoid leaf wetness, allowing photosynthesis to proceed during long wet periods by keeping stomata exposed to air (Field et al., 1998; Holder, 2007a; Aparecido et al., 2017). In seasonal rainforests, evergreen plants that rely on foliar uptake to survive the dry season (Yates and Hutley, 1995; Eller et al., 2013) must have leaves equally able to cope with a prolonged and intense rainy season when photosynthesis may be limited if water films cover stomata. In coast redwood (*Sequoia sempervirens* D. Don), the hydraulic benefits of foliar uptake (Burgess and Dawson, 2004) coexist with a capacity to maintain high wet-season stomatal conductance despite the nearly continuous presence of aerial water (Ambrose et al., 2010).

Sequoia maintains dominance in the presence of co-occurring conifers because it outlasts them by multiple lifespans (Sillett et al., 2021). The longevity and persistent growth of *Sequoia* supports the development of deep-canopied multispecies forests capable of attaining global maximum biomass and leaf area (Van Pelt et al., 2016; Sillett

et al., 2020). In addition to massive trunks and limbs, *Sequoia* invests in tannin-rich heartwood, fire-resistant bark, and pest-resistant leaves, all of which promote disturbance survival (Fritz, 1931; Clark and Scheffer, 1983; Davies et al., 2014). Additionally, leaf-level phenotypic plasticity allows tall *Sequoia* to optimize traits across deep crowns in response to environmental conditions, particularly water stress (Oldham et al., 2010; Van Pelt et al., 2016; Chin and Sillett, 2019). *Sequoia* exhibits all the indications of heteroblastic shoot development (Jones, 1999), characterized by abrupt (metamorphic) developmental transitions between thick, woody “axial” shoots with decurrent scale-leaves and the initially pliable “peripheral” shoots they support, which represent the vast majority of the total leaf area (Figure 1; Kramer et al. [2014] reported that woody shoots support ~5% of leaf area). The presence of these two distinct shoot types (dimorphism) is recognizable from their earliest growth. Each individual shoot apical meristem produces only one type, and differences are not due to age-related developmental shifts. Peripheral shoots may sometimes live to become stiff and woody, but they appear to be exclusively produced by separate meristems from those that originate axial shoots. Shoot dimorphism in *Sequoia* is separate from the broad, though gradual (allomorphic) changes seen with height among peripheral shoots (Koch et al., 2004; Oldham et al., 2010; Figure 1). While the ability



FIGURE 1 Peripheral and axial leaves of redwoods. Redwood shoots appear to be heteroblastic with an abrupt metamorphic change between dimorphic shoot types (transition visible in left panel). In panel on right, peripheral shoots (left column), which make up most leaf area, vary dramatically with height but always have less-decurrent leaves and are pliable during early years of development. Axial shoots (right column) are thick, woody, central shoot-cluster leaders supporting many peripheral shoots. They have highly decurrent leaves at all heights and never arise from peripheral-shoot meristems.

of redwoods to absorb water through leaves and improve tree water status is well documented (Burgess and Dawson, 2004), causes of variation in foliar uptake capacity remain untested experimentally. Specifically, analysis of within-crown variation in foliar uptake is missing, limiting our ability to identify environmentally responsive leaf traits regulating water absorption or to investigate the consequences of whole-tree foliar uptake across the broad geographic range of *Sequoia*. How does this species balance the contrasting requirements of water absorption and water repellency to flourish under wet or dry conditions? Variation in leaf interactions with water may have broad ecological implications, as the degree to which water is shed from, absorbed into, or evaporated off leaf surfaces influences forest hydrology, precipitation dependence, and drought susceptibility (Holder, 2007b; Konrad et al., 2012; Schreel and Steppe, 2020).

Foliar water uptake is driven by the Ψ gradient between the wet surface and interior of the leaf (Rundel, 1982). In obedience to Ohm's Law, hydraulic flux into the leaf should be proportional to the interaction between the Ψ gradient and hydraulic resistance at the leaf surface. The gravitational component of Ψ contributes approximately -1 MPa to the hydraulic tension at 100 m in a tall tree (Zimmermann, 1983), creating a natural gradient in the potential energy available to power treetop foliar uptake. However, foliar uptake rates do not always increase along the Ψ gradient (Limm and Dawson, 2010; Schreel et al., 2019), indicating that resistance can dominate the system. Wide variation in foliar water uptake among plant species (Limm et al., 2009; Gotsch et al., 2015; Emery et al., 2016; Guzmán-Delgado et al., 2018; Schreel et al., 2019) is evidence that while the Ψ gradient may be the force driving uptake, leaf features determine its maximum rate. In contrast to Ψ , variation in leaf-surface hydraulic resistance is most likely determined by a suite of factors that can respond to the local environment given adequate plasticity. Leaf surface traits that may confer hydraulic resistance are most likely those related to surface-water interactions, such as stomatal density and size, structure of epicuticular waxes and cuticle, and stomatal plugs (Field et al., 1998; Rosado et al., 2010; Aparecido et al., 2017; Guzmán-Delgado et al., 2018; Kerhoulas et al., 2020). These surface traits can change with crown position (Rosado et al., 2010; Chin and Sillett, 2019) and, in *Sequoia*, may be different between dimorphic shoot types (Figure 1). The potential for variability in foliar uptake capacity between shoot types leads us to hypothesize that availability of local resources (light and aerial water) may control development of shoot morphotypes and their plasticity, separating the tasks of foliar uptake and photosynthesis.

Sequoia thrives in seasonally dry, coastal rainforests and much drier forests farther south and distant from the ocean, where it tolerates hot, dry summers and survives infrequent but severe droughts. The goals of this study were to explore how foliar uptake in *Sequoia* is balanced with the primary photosynthetic function of leaves and identify the traits

causing resistance to water absorption. We suspected that shoot dimorphism in *Sequoia* provides a means of maximizing wet-season carbon acquisition while acquiring atmospheric water; however, the existence of heteroblasty in this species requires anatomical and physiological validation. Shoot dimorphism may afford an opportunity to separate functionally exclusive leaf traits promoting either water uptake or permitting photosynthesis on wet days. Furthermore, we expect that the within-crown and geographic distribution of peripheral and axial shoots will reflect their potential functional division. If aerial water accessibility is determined by leaf traits that change surface hydraulic resistance, then leaf structural variation will influence foliar uptake capacity independent of the Ψ gradient. To evaluate the broader significance of foliar uptake to *Sequoia* function, we made the first whole-crown estimates of foliar water uptake capacity for any tree, using some of the largest trees known. We measured foliar water uptake by peripheral and axial shoots collected across the vertical distribution of *Sequoia* foliage, scaled-up by branch- and tree-level allometry (Kramer et al., 2014; Sillett et al., 2015, 2020), to quantify foliar uptake and reveal its potential contributions to whole-tree water balance and forest hydrology.

MATERIALS AND METHODS

Experimental methods and trait measurement

Measurement of leaf traits

We collected a total of 16 small *Sequoia* shoot clusters from six trees at five climatically distinct forest locations (latitude 36° to 41°N; Tables 1, 4) that yielded high trait diversity (Table 2). We also estimated potential whole-crown uptake rates for an additional seven trees (see Table 4), including the tallest living individual, to explore the diversity of *Sequoia* crown structure. Samples from the six study trees were collected at heights from 22 to 102 m above ground level, between December 2018 and March 2019 (before spring leaf-out). Within each sample cluster (also used for experimental fogging), we separated leaves on peripheral and axial shoots for purposes of trait analysis (Figure 1). Samples used for experimental fogging were large and made up of multiple shoots, representing the full age range of each shoot type. For trait analyses, we used the most recent growth available. Our measurements combined traditional anatomical cross sections, acrylic imprints, and high-resolution composite macroimaging to characterize leaf traits. While our emphasis was on the effects of surface traits, we also compared the vascular anatomy of peripheral and axial leaves to understand their functional roles (Table 2). We fixed fresh peripheral and axial leaves in FPA (10:5:50:35 formalin, propionic acid, 70% ethanol, and distilled water), embedded them in paraffin, and cut 10- μ m thick cross sections using a rotary

TABLE 1 Sets of variables used in this study with data sources and locations ranked by latitude. Climatic data are 30-yr monthly means 1981–2010 with 800-m spatial resolution, dew point is maximum temperature (temp.) for condensation, VPD is vapor pressure deficit (climatic data from PRISM Climate Group, 2020).

| Variables | | Data sources | Previous publication | | N | | | |
|------------------------------|-----------|--|--|-----------------------------------|------------------------------------|-----------------------|----------------------|-----------------------|
| (A) Leaf traits in Table 2 | | All 11 traits are from the current study | None | | 6 trees, 5 locations, see Table 2 | | | |
| (B) Predicted photosynthesis | | Both sources used the same 5 trees from 1 location; we used the combined data to estimate the output of lateral leaves at different heights. | | | | | | |
| Light response curves | | Mullin et al. 2009 | Summary data for 3 height-bins | | 14 heights, 3 curves each | | | |
| Light availability | | Oldham et al. 2010 | Points shown, equation not provided | | 57 crown positions | | | |
| (C) Leaf area fractions | | Sillett et al. 2010, 2015; Kramer et al. 2014 | Total leaf area, not lateral/axial fractions | | 93 branches, 43 trees, 7 locations | | | |
| Location | Variables | Latitude | Annual rainfall (mm) | Mean monthly summer rainfall (mm) | Mean summer dew point (°C) | Min summer temp. (°C) | Max summer VPD (hPa) | Max summer temp. (°C) |
| JS ^a | A, C | 41.8 | 2003 | 25 | 11 | 10 | 14 | 22 |
| PC ^a | C | 41.4 | 1648 | 19 | 10 | 9 | 11 | 21 |
| RNP ^a | C | 41.2 | 1757 | 20 | 11 | 10 | 14 | 23 |
| HR ^a | B, C | 40.3 | 1722 | 11 | 10 | 10 | 28 | 29 |
| RRR ^b | A | 38.6 | 1356 | 4 | 11 | 11 | 21 | 25 |
| ATP | A | 38.4 | 1100 | 3 | 9 | 12 | 29 | 29 |
| SPT ^b | C | 38.0 | 1061 | 3 | 11 | 11 | 21 | 26 |
| RRP ^c | A | 37.8 | 727 | 3 | 10 | 12 | 19 | 25 |
| BB ^b | C | 37.2 | 898 | 4 | 11 | 11 | 21 | 27 |
| SCM ^b | A | 37.1 | 1487 | 4 | 8 | 14 | 24 | 27 |
| LH ^c | C | 36.1 | 868 | 2 | 9 | 12 | 20 | 24 |

^aNorthern site.

^bCentral sites.

^cRange margins.

microtome. After staining slides with methylene blue and safranin, the vascular bundle (xylem, transfusion tissue, phloem, and fibers) was photographed at 20×. To verify that the phloem structural differences were not artifacts of slide preparation, we examined additional fresh green sections of axial leaves. We prepared acrylic resin (nail polish) imprints of the adaxial and abaxial leaf surfaces and photographed them at 10× for measuring stomatal density and 40× for measuring guard cell length. Because guard cell length is strongly correlated with stomatal pore area (Lawson and Matthews, 2020), it serves as a reliable index for stomatal covering fraction (stomatal pore area per leaf area). Further, we measured the fraction of the leaf covered with visible epicuticular waxes (wax area per leaf area) and documented the area-based distribution of epiphyllic organisms (absent from peripheral shoots) using composites created from stacked macroimages of adaxial and abaxial leaf surfaces taken at slightly different focal depths to create seamless high-resolution surface images (Figure 2A, B). We verified that the white substances photographed (Figures 2A, 3B) were

epicuticular waxes by dipping leaves in chloroform, which retains any (potentially white) fungi on the leaf but removes wax. We were unable to measure adaxial surface traits for axial leaves because of a heavy covering of epiphyllic organisms (Figure 2B). All images were analyzed with Fiji ImageJ (National Institutes of Health, Bethesda, MD, USA).

Although the phloem anatomy of axial leaves is not indicative of a photosynthetic contribution (Figure 2C, D), to verify functional differences, we measured mid-morning (10:00–11:00 hours) photosynthesis and stomatal conductance on sets of peripheral ($N = 5$) and axial ($N = 7$) shoots reachable from ground level in five *Sequoia* trees on the UC Davis campus. We recognize that measurements of photosynthesis are related to sample collection height (Mullin et al., 2009), but we assume that physiological differences between axial and peripheral shoots will hold across the crown, as their structural dissimilarities remain consistent. We assume here that for a given microclimatic condition the pairwise differences

TABLE 2 Definitions of foliar traits used in this study and their values and differences between peripheral and axial shoots of *Sequoia sempervirens*. Surface traits are for abaxial side of leaf; large errors around means reflect broad morphological diversity of *Sequoia* leaves (see Figure 1). All eight surface and vascular traits are also used in PCA. Values in parentheses indicate 1 SE of estimate expressed as a percentage. *W* is the test statistic from the Wilcoxon rank sum tests. *N* = 10 peripheral and 10 axial samples.

| Trait | Definition | Unit | Peripheral Mean \pm SE | Axial Mean \pm SE | <i>W</i> | <i>P</i> |
|---------------------------------------|-----------------------------------|---------------------|--------------------------|---------------------|----------|----------|
| Physiological | | | | | | |
| Initial surface permeability to water | Maximum instantaneous uptake rate | g/m ² | 7.14 (14) | 23.79 (15) | 129 | <0.0001 |
| Surface | | | | | | |
| Visible wax coverage | Wax area per leaf area | fraction | 0.5625 (13) | 0.2338 (15) | 143 | 0.0019 |
| Guard cell length | Mean guard cell length | mm | 0.0352 (5) | 0.027 (10) | 104 | 0.0169 |
| Stomatal density | Stomata per leaf area | no./mm ² | 48.88 (12) | 36.03 (18) | 91 | 0.1151 |
| Guard cell covering fraction | Guard cell length per leaf area | mm/mm ² | 1.6734 (12) | 0.9639 (21) | 102 | 0.0210 |
| Vascular | | | | | | |
| Transfusion tissue area | Cross-sectional area | mm ² | 0.0127 (9) | 0.0207 (14) | 22 | 0.0065 |
| Xylem area | Cross-sectional area | mm ² | 0.0028 (7) | 0.0018 (11) | 107 | 0.0100 |
| Phloem area | Cross-sectional area | mm ² | 0.0032 (9) | 0.0021 (19) | 102 | 0.0234 |
| Central fibers | Number per cross section | no. | 0.62 (53) | 3.1 (16) | 16 | 0.0016 |

TABLE 3 Equations developed for approximations of *Sequoia sempervirens* whole-crown foliar uptake and photosynthetic potential. RMSE, root mean square error; CV, coefficient of variation (RMSE/mean) expressed as a percentage. Uptake equations have weak predictive ability; however, they have significant slopes, making them generally preferable to mean values for our tree-level estimates and allow us to consider the impact of the vertical Ψ gradient and the distribution of peripheral and axial leaf area in a way that mean uptake values would not.

| Dependent variable | Predictor (<i>V</i>) | <i>a</i> | <i>b</i> | <i>N</i> | <i>R</i> ² | RMSE | CV | <i>P</i> | Form |
|--|------------------------|----------|----------|----------|-----------------------|-------|-----|----------|----------------|
| % Axial leaf area, locations north of 40° | Relative height | -4.7753 | 9.0622 | 54 | 0.25 | 1.667 | 30 | 0.0001 | $aV + b$ |
| % Axial leaf area, southernmost location (LH) | Relative height | 7.907 | 2.097 | 12 | 0.44 | 0.978 | 13 | 0.0193 | $aV + b$ |
| Photosynthetic potential ($\mu\text{mol CO}_2 \text{ m}^{-2}\cdot\text{s}^{-1}$) | Relative height | 7.3679 | 10.853 | 14 | 0.74 | 1.440 | 19 | <0.0001 | $a \ln(V) + b$ |
| Axial-leaf water uptake ($\text{g H}_2\text{O m}^{-2}\cdot\text{min}^{-1}$) | Initial Ψ (MPa) | 0.45585 | - | 58 | 0.60 | 0.237 | 91 | <0.0001 | $aV + 0$ |
| Peripheral-leaf water uptake ($\text{g H}_2\text{O m}^{-2}\cdot\text{min}^{-1}$) | Initial Ψ (MPa) | 0.09708 | - | 174 | 0.26 | 0.104 | 185 | <0.0001 | $aV + 0$ |

between axial and peripheral shoots would be consistent, particularly because peripheral shoots lacked visible epiphyllic organisms at all heights, and axial shoots never had phloem that appeared capable of sugar export. Without detaching shoots from trees, we analyzed each at ambient light and 400 ppm CO₂ with a Li-6400 portable photosynthesis meter (LI-COR, Lincoln, NE, USA) equipped with a conifer chamber, deliberately choosing neighboring peripheral and axial shoots in both sun and shade. We then removed the shoots and dissected them to determine fresh area. Although we did not compare shoot Ψ in this case, before equilibration in the dark, peripheral shoots collected for fogging tended to have slightly more negative water potentials (~ 0.1 – 0.01 MPa lower) than axial shoots in the same cluster, so we do not believe they were under less tension here.

Measurement of foliar uptake

After collection, sampled shoot clusters were recut under water and allowed to rehydrate completely before beginning measurements. In the lab, the woody ends of each shoot cluster were recut in melted paraffin to create a seal (Chin and Sillett, 2016) before bench-drying to within ± 0.03 MPa of the estimated pre-dawn maximum Ψ for their collection height based on the gravitational potential gradient. Bench-dried samples were kept cool overnight in a sealed dark bag to enable equilibration of Ψ throughout the shoot cluster, which was later verified with a pressure chamber before beginning the fog exposure treatment. Our sample size was limited by the need to work with shoots within a few days of collection and to dry hydrated samples down to a narrow Ψ range. Unfortunately, we could not use some sample

TABLE 4 Individual *Sequoia sempervirens* trees used for measurements of physiological and anatomical traits of peripheral and axial shoots (Variable A, Table 1). Trees varied widely in size and age; *f*-DBH is functional diameter at breast height (1.37 m). Size metrics were estimated from existing allometric equations. Whole-crown foliar water uptake and photosynthetic potential (peripheral leaves only) were approximated using equations in Table 3; these uptake estimates apply to the first hour of fog exposure only. Axial uptake contribution is the percentage of whole-crown uptake contributed by axial leaves. Location details are in Table 1. Trees A–F (in bold) were sampled for fog exposure; additional trees are shown to explore foliar uptake across the diversity of tall-redwood crown structure. Values in parentheses indicate 1 SE of estimate expressed as a percentage.

| Tree | Location | Height (m) | <i>f</i> -DBH (cm) | Crown volume (m ³) | Tree age (yr) | Tree biomass (Mg) | Projected leaf area (m ²) | Leaves (millions) | Axial leaf area (%) | Estimated foliar uptake (kg H ₂ O/h) | Estimated photosynthetic potential (kg CO ₂ /h) | Axial uptake contribution (%) |
|------|----------|-------------|--------------------|--------------------------------|---------------|-------------------|---------------------------------------|-------------------|---------------------|---|--|-------------------------------|
| A | JS | 97.9 | 750 | 25085 | 1261 (9) | 350 (4) | 8834 (18) | 1004 (17) | 5.8 | 48 | 10 | 20 |
| B | RRR | 93.9 | 276 | 11155 | 543 (7) | 54 (4) | 2916 (18) | 297 (18) | 8.0 | 16 | 3 | 27 |
| C | RRR | 98.2 | 212 | 7402 | 650 (2) | 38 (4) | 2087 (17) | 209 (17) | 8.0 | 13 | 3 | 27 |
| D | ATP | 70.2 | 184 | 3586 | 238 (7) | 17 (4) | 2056 (16) | 193 (16) | 7.9 | 9 | 3 | 27 |
| E | RRP | 64.0 | 129 | 1380 | 148 (2) | 10 (4) | 929 (18) | 95 (17) | 8.3 | 4 | 1 | 28 |
| F | SCM | 107.3 | 352 | 15016 | 874 (1) | 94 (4) | 2268 (32) | 228 (32) | 8.0 | 24 | 4 | 27 |
| G | JS | 108.4 | 420 | 7924 | 885 | 146 | 4527 (6) | 481 (5) | 5.5 | 28 | — | 19 |
| H | JS | 97.0 | 558 | 17142 | 1278 | 231 | 5234 (5) | 558 (4) | 7.3 | 33 | — | 25 |
| I | PC | 102.7 | 680 | 18041 | 1142 | 251 | 6959 (6) | 729 (5) | 6.7 | 44 | — | 23 |
| J | RNP | 115.9 | 495 | 12675 | 908 | 197 | 5193 (6) | 555 (6) | 3.9 | 30 | — | 14 |
| K | RNP | 113.0 | 425 | 14616 | 1900 | 144 | 3722 (5) | 406 (3) | 3.8 | 22 | — | 14 |
| L | RNP | 109.4 | 493 | 12040 | 773 | 198 | 6641 (6) | 725 (5) | 5.4 | 40 | — | 19 |
| M | HR | 113.0 | 364 | 11051 | 829 | 113 | 4036 (6) | 436 (6) | 4.7 | 24 | — | 17 |

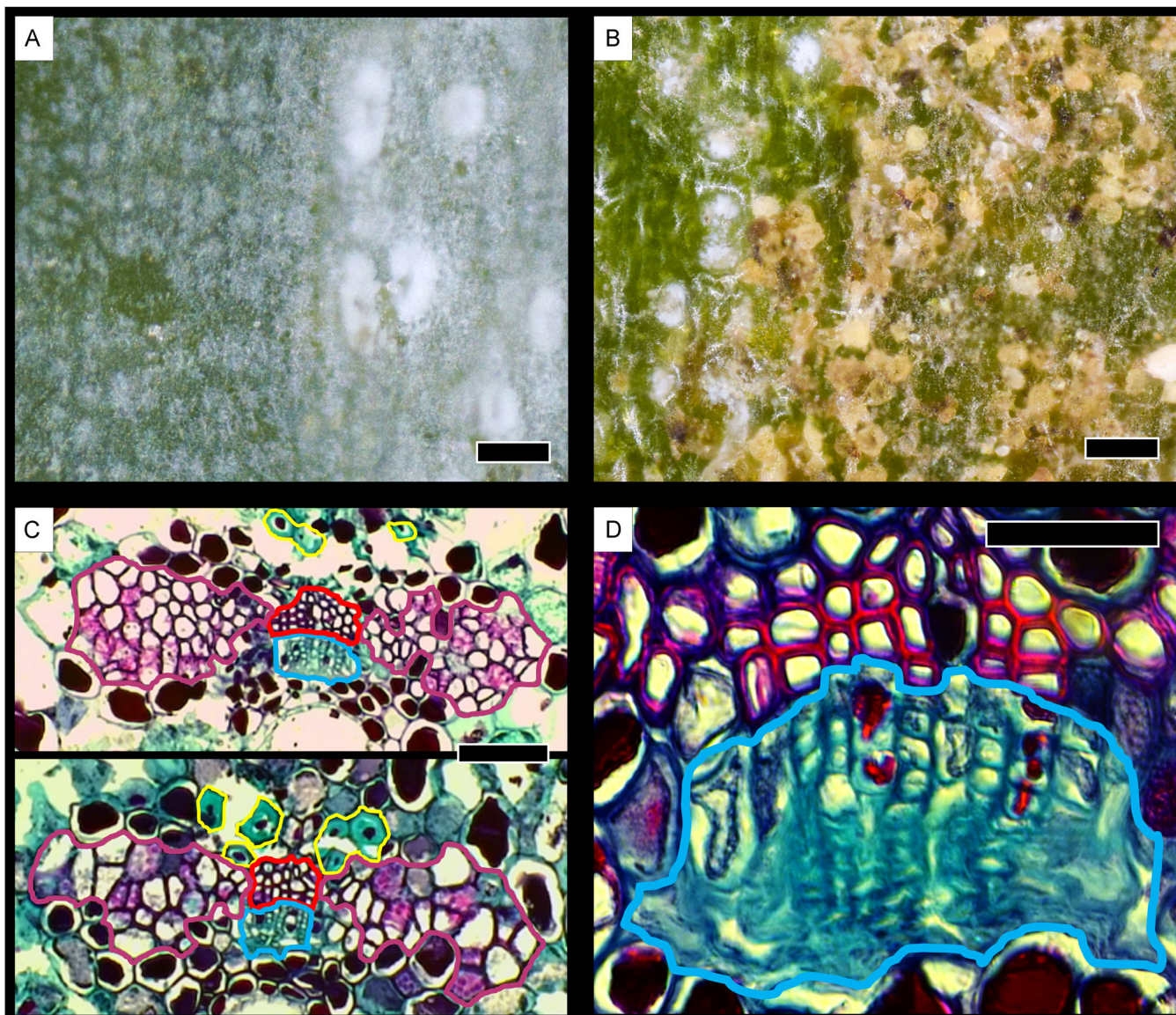


FIGURE 2 Traits of peripheral and axial leaves. (A) Waxy abaxial surface of peripheral leaves showing stomatal plugs (white spots). Scale bar = 0.05 mm. (B) Sheltered adaxial surfaces of axial leaves host abundant epiphyllic organisms, having >70% cover in our samples. Scale bar = 0.05 mm. (C) Vascular anatomy of peripheral leaves (top) and axial leaves (bottom). Outlines: purple = transfusion tissue, yellow = central fibers, red = xylem, blue = phloem. Scale bar = 0.1 mm. (D) Phloem of axial leaves (blue outline) has many occluded cells and fused walls, suggesting reduced sugar-transport functionality. Scale bar = 0.035 mm.

clusters because we failed to hit their target pre-dawn Ψ . The time and difficulty involved in the experiment, and especially our use of fresh shoots, required spreading sampling over five tree-climbing expeditions, collecting a maximum of four shoot clusters each time.

To capture the full range of leaf development and age distribution, we removed all undamaged individual shoots bearing either peripheral or axial leaves per sample cluster with an estimated maximum age of peripheral shoots (based on node counts) from 1–7 yr and of axial shoots from 1–12 yr. We included all green shoots on a cluster regardless of size or age, only excluding those with obvious damage, although leaf traits were measured on current-year shoots

only. Cut ends of individual shoots were sealed with Parafilm, then the entire shoot was briefly submerged and blotted dry before weighing, which helped ensure that more appressed treetop-peripheral and -axial leaves were dried to the same level both before and after fogging, regardless of water retained in crevices. To be certain that any error introduced by retained water was negligible, we selected 10 diverse redwood shoots and weighed them dry, and following our wetting and blotting method, found a mean weight increase of only 0.23% (SD = 0.22%) as a result of unremoved water. We thus expect that the pre-wetting and blotting procedure removed what would have been ~3% error between samples weighed completely dry and those

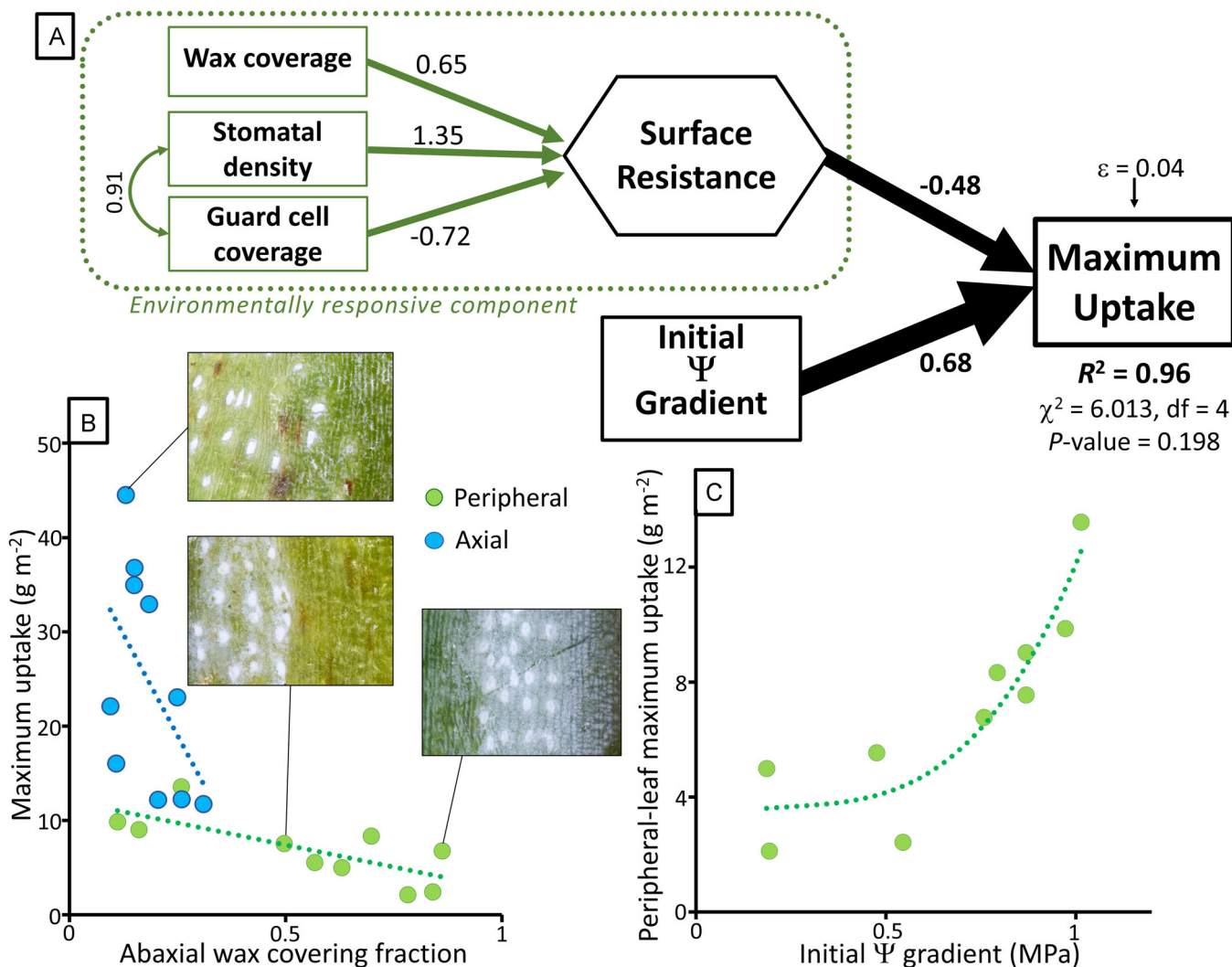


FIGURE 3 What causes variation in foliar uptake potential? (A) Based on Ohm's Law, this structural equation model characterizes our determination of peripheral-leaf initial surface permeability, or "maximum uptake", by leaf surface resistance and Ψ gradient (mimicking the predawn Ψ gradient due to gravity). Black arrow thickness shows relative effect sizes. Surface resistance is caused by composite effects of three leaf traits (green arrows). Dotted green box designates portion of model that may respond to environmental signals through acclimation or long-term regional adaption of leaf traits. Arrows indicate directions of causality. Small curved green arrow (far left) represents covariance of stomatal density and guard cell coverage (trait definitions in Table 2). Path coefficients are relative effect sizes in units of standard deviation. Surface resistance and the initial Ψ gradient are conditionally independent; thus, when controlling for Ψ , surface traits explain nearly all variation in initial surface permeability (maximum uptake). (B) Relationship between abaxial wax covering fraction and uptake rate in peripheral leaves ($R^2 = 0.56$) and axial leaves ($R^2 = 0.26$). Insets show leaf surfaces; white substances are waxes. (C) In peripheral, but not axial, leaves maximum uptake increases with magnitude of initial Ψ gradient ($R^2 = 0.85$).

weighed after fog exposure and blotting; however, within-sample error from inconsistent post-blotting water retention was likely far lower than the difference between blotted-dry and completely-dry shoots. Using the method of Guzmán-Delgado et al. (2018), we suspended shoots in a fog-filled chamber in their natural orientations and removed at ~ 20 -min intervals to allow for determination of temporal dynamics in foliar water uptake (mean fogging time = 132 min). Fogged shoots were immediately blotted dry and weighed as before, and their final Ψ was recorded. After fogging, each shoot was carefully dissected and scanned to quantify leaf silhouette area. The series of pre- and post-fog-exposure measurements of mass per area and

Ψ were used to generate curves to determine the foliar uptake rate as a function of initial water potential per sample.

Data analyses

Comparison of peripheral and axial leaves

To examine the differences between peripheral and axial leaves, we used principal component analysis (PCA) of eight untransformed foliar traits (Table 2). The PCA was performed on peripheral and axial leaves together using a

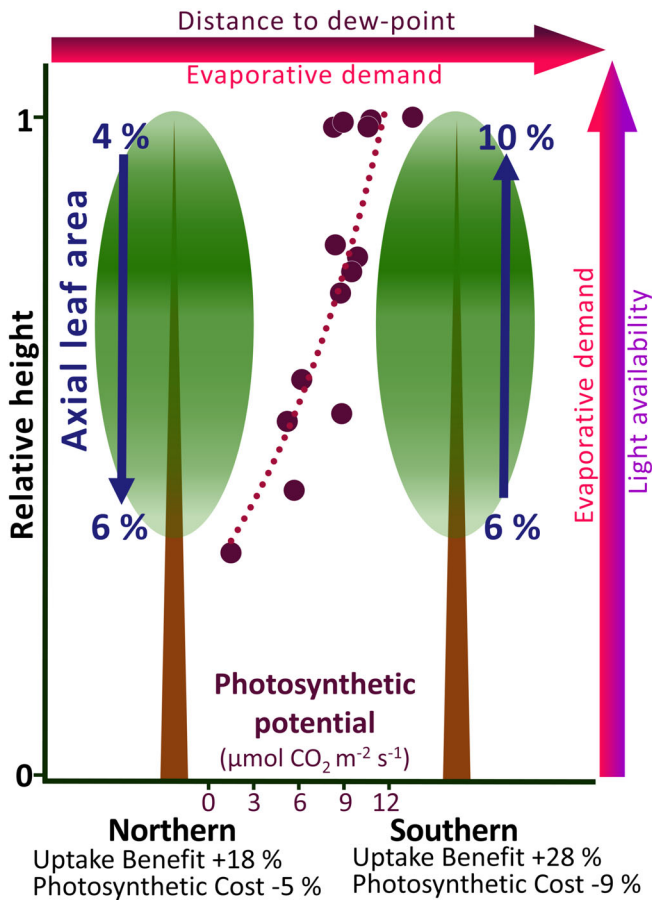


FIGURE 4 Geographic variation in foliar water uptake requirements and axial shoot distribution. Conceptual model illustrating how multiscale environmental variation within and among *Sequoia* forests could necessitate prioritization of axial leaf area in upper crowns of trees growing in southern range. In treetops, axial leaves have their greatest cost in lost peripheral-leaf photosynthetic opportunity but also make their greatest uptake contribution relative to peripheral leaves. Increased distance between minimum summertime temperatures and dew point, and near absence of measurable precipitation, indicate that southern forests have less frequent summertime leaf wetting events compared to northern forests (Table 1). Greater evaporative demand at southern and eastern range margins suggests that these infrequent condensation events are sustained for shorter periods, while vertical gradients in evaporative demand imply that treetops experience the shortest leaf-wetting events. Taking full advantage of rare and transient leaf wetness—to allow hydraulic repair despite the gravitational Ψ gradient—could explain the relatively high treetop axial fraction in southern forests and supports the notion that ability to improve water status has a positive effect on CO_2 acquisition. Using centrally located tree C (latitude 38.6° , Table 4) as an example, we show estimated axial leaf areas for northern trees ($>40^\circ$ latitude) and southern trees (LH location, 36° latitude, Table 1). Color shading of tree crowns indicates the relativized distribution of tree C's total leaf area in 5-m height bins. Photosynthetic potential is estimated from in situ light availability for purposes of discussion but is not corrected for within-crown gradients in Ψ or latitudinal variation in solar angle. Approximate benefit from axial-shoot foliar water uptake and CO_2 lost-acquisition cost shown below compared to a peripheral-only scenario (values generated from equations in Table 3).

correlation matrix with Euclidean distance. The mean trait skewness was 0.679 and mean kurtosis was 0.683 with all individual-trait values below three. The R package hyper-volume (Blonder, 2018) was used to measure the overlap of

peripheral and axial leaves in trait space based on PC axis scores. We tested whether uptake rates, traits, and photosynthetic rates were dependent on leaves being peripheral or axial using Wilcoxon rank sum tests with continuity correction for ties via R 3.4.3 (R Core Team).

Quantification of foliar water uptake rates for whole-tree scaling

With data from the fogging experiment, we plotted area-based mass increase per minute ($\text{g} \cdot \text{m}^{-2} \cdot \text{min}^{-1}$) against the initial Ψ of each shoot in a cluster when first exposed to fog, forcing the line through the origin to reflect the lack of uptake in the absence of a Ψ gradient. The resulting linear fits (Table 3) were used with estimates of peripheral and axial leaf areas to predict uptake in 5-m foliar-height bins using the assumed pre-dawn Ψ (e.g., -0.98 MPa at 100 m). These values were established per shoot cluster at their individually estimated pre-dawn Ψ , so we assume they reflected uptake under natural conditions in the tree and preserved the impacts of vertical gradients in foliar traits. We estimated whole-tree uptake over the first hour following fog exposure. Shoots were typically exposed to fog for >2 h and saw increases in Ψ greater than would be expected if attached to a tree. Therefore, it is likely that we underestimated the first-hour uptake potential. However, we chose 1 h as the time for estimation because we have no information on how Ψ changes in shoots attached to large-capacity trees during fog exposure. We expected that the realized Ψ increases are small over this initial time period.

Whole-tree scaling and leaf-type distribution

Previous research on *Sequoia* involved intensive mapping of tree crowns and dissection of representative samples in both unlogged primary forests and previously logged secondary forests (Sillett et al., 2010, 2015, 2018; Kramer et al., 2014). In these studies, estimates of leaf area were reported as total leaf area, but during branch dissections of foliage, pliable shoots were measured separately from woody shoots along the height gradient. All leafy twigs up to 1 cm in diameter were separated into three categories: young pliable shoots bearing green leaves (L), older woody shoots bearing green leaves (G), and woody shoots bearing mostly brown leaves (B). In the present study, we used the L category to estimate peripheral leaf area, and we averaged G and B categories to estimate axial leaf area per branch. These estimates of peripheral and axial leaf areas afforded us opportunities to consider them separately in a scaling exercise and to assess the physiological and ecological implications of their distributions within and among trees growing in different forests. For purposes of whole-tree scaling, we estimated peripheral and axial leaf areas in 5-m height for individuals sampled in this study. Equations for estimating peripheral and axial leaf area fractions were developed for trees in

northern and southern primary forests based on previous branch dissections (Table 3; Kramer et al., 2014; Sillett et al., 2015). We applied allometric equations to predict total leaf area per height bin, which were developed by crown mapping 114 trees in primary forests (Sillett et al., 2020). We also estimated total peripheral and axial leaf area for an additional six crown-mapped trees up to 116 m tall.

Estimates of leaf area were used to predict water uptake of peripheral and axial leaves per 5-m height bin. To investigate the photosynthetic cost of axial leaf investment, we combined existing data on light attenuation with depth in *Sequoia* crowns (Oldham et al., 2010; $N = 5$ trees, 57 inner and outer crown positions) and the photosynthetic response to light availability from peripheral leaves collected at different heights in the same trees (Mullin et al., 2009; $N = 5$ trees, 14 crown positions). For each of the 14 samples with light curves, we predicted peripheral-shoot photosynthetic output based on local light availability, though these curves were established for hydrated shoots. This approach enabled us to generate a logarithmic curve (Table 3, Figure 4) to approximate the leaf-area-based photosynthetic potential per height bin for peripheral leaves. This curve is for purposes of interpreting the relative distributions of axial and peripheral leaf area, but it ignores the impacts of the natural Ψ gradient, which would lower in situ photosynthetic rates and presumably bring treetop photosynthetic contributions closer to those of the lower crown. We used area-based, rather than mass-based estimates for photosynthetic assimilation (A) because foliar water uptake was measured on an area basis. Our calculations assume that axial shoots have a neutral carbon balance. Although our photosynthetic measurements suggest a slight axial-shoot cost (less photosynthesis than respiration), due to a lack of data on in situ photosynthetic parameters, we chose this as a more conservative approach.

Quantification of initial surface permeability for trait models

Modeling impacts of leaf traits on foliar water uptake required establishment of sample-specific uptake capacities for comparison. Using mass increase and shoot area data from the fogging experiment, we established an “initial surface permeability” value per sample by plotting water absorption ($\text{g}\cdot\text{m}^{-2}$) against number of minutes each shoot was exposed to fog for sets of peripheral and axial shoots per sample. We did not use any experimental runs with initial mass losses $>10\%$ because we assumed experimenter error (2 runs) and discarded 6 of 248 individual points as outliers based on Cook's distance before fitting logarithmic curves. Only multishoot curves yielding rates with errors less than the estimates, along with complete sets of trait data, were retained (final curves: $N = 10$ peripheral, 10 axial). For each sample-specific function [Form: $y = m \ln(x) + b$], we used the first derivative at “minute one” [form: $y' = m (1/x)$] as “initial surface permeability” ($\text{g}\cdot\text{m}^{-2}$). These initial surface

permeability values, derived from functions specific to shoots per sample cluster, indicate potential maximum uptake rate at the start of foliar water absorption, but they do not reflect continuous uptake of water over time (uptake rate), making them unsuitable for estimates of whole-tree uptake, for which we used equations in Table 3.

Structural equation models explaining initial permeability

A typical goal of structural equation modeling (SEM) is to test the validity of an a priori theoretical model by examining how well it approximates relationships (covariance) in a matrix of observations. The assumption that the model is correct (based on knowledge of the system) allows users to estimate the relative causative effects of factors influencing a variable of interest (Grace, 2006). In our case, if uptake is a purely physical process, then the underlying model explaining variation in foliar uptake is Ohm's Law. Rather than testing the validity of this law of physics, we had the potential to fit a fundamentally correct model. Our first goal was to estimate conditionally independent effect sizes of surface resistance and $\Delta\Psi$ on uptake rate by specifying a model for uptake with paths from initial $\Delta\Psi$ and a composite variable representing “surface resistance” (Figure 3A). This modeling approach allowed us to identify a set of traits whose collective effects determine surface resistance. Because the a priori model is Ohm's Law, using prior knowledge of trait function to identify a combination of leaf surface properties resulting in a good-fitting covariance matrix helped to establish a causal relationship between surface traits and hydraulic resistance.

We selected candidate leaf traits from both the adaxial (peripheral leaves only) and abaxial leaf surfaces to create potential composite variables representing surface resistance in an iterative, leave-one-out approach (surface traits in Table 2). Beginning with a saturated model containing four traits per leaf side, we removed the worst performing trait per step, adding a trait back in and trying another if its removal decreased model quality. The final model structure for peripheral leaves was selected because it was the only model where (1) all traits had significant parameters with errors $\leq 50\%$ of the estimates and (2) R^2 , χ^2 , sample-size-corrected Akaike information criterion (AIC_c), and comparative fit index (CFI) all suggested an adequate fit (Grace, 2006). In most cases, the SEM process relies on a large sample size to obtain model fit. Here, we were able to fit a small sample-size model (i.e., $N = 10$ peripheral leaf uptake values) because of the unusual circumstance of having a simple, substantially over-identified recursive model with no latent variables, exogenous variables all with very low measurement error, strong correlations with maximum uptake, and perhaps most importantly, a physical law as an a priori model. Unfortunately, where modeling was unsuccessful (as for axial shoots), we could not conclude that it was because the specified process (Ohm's Law) did not describe the observed

data. Our goal was to understand a process and locate causes of resistance, not to make predictions based on the parameter estimates, so the inability to calculate a reliable root mean square error of association (RMSEA) at small sample sizes was not problematic.

As part of our compositing process for the “surface resistance” variable, we specified the loading for the first-listed trait causing resistance in each candidate composite. These start values were obtained by first specifying a SEM model where initial surface permeability was directly predicted by traits selected for defining the new composite variable. We then pre-multiplied the parameter estimate from that initial model by the first-listed trait in the candidate composite variable to specify its start estimate (Grace, 2006). Since both leaf structure and maximum Ψ are height-associated, we examined impacts of shared causality (from sample height) between traits and Ψ , and we re-fit the single retained model, removing Ψ , and adding height as a predictor of uptake as well as each of the three traits causing resistance. We used maximum likelihood estimators to obtain model fits, and we assessed global and local model fits and complete specification of relationships in models with R^2 , χ^2 , AIC_c, CFI, and examination of residuals (Grace, 2006). This SEM process was repeated for peripheral leaves, axial leaves, and both together, but it was only successful for peripheral leaves, retaining three leaf traits as the causes of surface resistance. We report path coefficients in units of standard deviation change to indicate their relative effect sizes. The R package lavaan was used for all SEM model specification, fitting, and calculation of fit measures (Rosseel, 2012). All statistical analyses were performed in R, and calculations were done in R and Excel (Microsoft, Redmond, WA, USA).

RESULTS

Comparison of peripheral and axial leaves

Principal component analysis of eight foliar traits yielded two significant axes, retaining 62% of the variation in peripheral and axial leaf structure. Within the full leaf-trait space, the separate eight-dimensional hypervolumes occupied by peripheral and axial leaves had zero spatial overlap, confirming that they belong to two entirely different shoot morphotypes easily distinguishable on the basis of surface and vascular traits without information on morphology or shoot position. The first principal component (PC1) correlated well with uptake rate ($R^2 = 0.45$) but only weakly with sample height ($R^2 = 0.12$). However, when considering points associated only with peripheral leaves, PC1 was strongly related to sample height ($R^2 = 0.82$) and uptake ($R^2 = 0.69$). Univariate differences in key vascular traits were suggestive of functional divergence. Peripheral leaves had greater xylem and phloem areas but less transfusion tissue and fewer central fibers than axial leaves (Figure 2C, Table 2). Phloem of axial leaves appeared largely

nonfunctional with either occluded cells or, in many cases, cell walls that had grown inward and filled lumens (Figure 2D).

We found that while peripheral leaves were photosynthetic as expected ($4.22 \pm 20\%$, $\mu\text{mol of CO}_2 \text{ m}^{-2} \text{ s}^{-1}$), axial leaves respired slightly more CO_2 than they assimilated in sun or shade ($-0.199 \pm 69\%$, $\mu\text{mol of CO}_2 \text{ m}^{-2} \text{ s}^{-1}$, $W = 35$, $P = 0.0025$), and only one of seven axial shoots exhibited positive net photosynthesis. Peripheral leaves also had stomatal conductance rates higher than those of axial leaves (peripheral: $0.0339 \pm 20\%$ mol of $\text{H}_2\text{O m}^{-2} \cdot \text{s}^{-1}$, axial: $0.0155 \pm 28\%$ mol of $\text{H}_2\text{O m}^{-2} \cdot \text{s}^{-1}$, $W = 30$, $P = 0.0480$). These photosynthetic results are presented with the caveat that they were not collected from tall trees in the field. However, all axial leaves sectioned in this study had apparently nonfunctional phloem and low stomatal density, and we have no reason to believe that they would be more photosynthetic under shadier, wetter deep crowns where epiphyllic organisms would presumably be more abundant on leaf surfaces. Additional research on this subject could prove interesting and potentially uncover a carbon cost to axial-shoot retention in tall *Sequoia*.

Whole-tree uptake scaling and shoot type distribution

Peripheral leaves were capable of foliar water uptake at a mean rate of $0.12 \text{ g} \cdot \text{m}^{-2} \cdot \text{min}^{-1} \cdot \text{MPa}^{-1}$, while axial leaves could absorb $\sim 4\times$ that amount, $0.48 \text{ g} \cdot \text{m}^{-2} \cdot \text{min}^{-1} \cdot \text{MPa}^{-1}$. We used equations in Table 3, however, rather than these mean values to estimate whole-crown uptake because they encompass the natural gradients in leaf structure and Ψ . The largest tree from which we collected shoots for fogging, which was 97 m tall with 8834 m^2 of leaf area distributed across a complex crown, had the potential to absorb $\sim 48 \text{ kg H}_2\text{O h}^{-1}$ at predawn Ψ during the first hour of water exposure, if the entire crown was wet (Tree A; Table 4). The smallest tree in our study, Tree E, which had 929 m^2 of leaf area distributed across a simple crown structure, had the potential to absorb $\sim 4 \text{ kg H}_2\text{O h}^{-1}$. The contribution of axial shoots to water uptake varied among trees (Table 4) and reached up to 28% of total foliar water uptake in dry inland forests with even greater fractional contributions in tree-tops. Among the seven additional trees (not used for experimental fogging) for which we estimated peripheral and axial leaf areas, estimated uptake increased with functional trunk diameter ($f\text{-DBH}$, $R^2 = 0.69$) due to an increase in both total leaf area and axial fraction ($R^2 = 0.45$) with this measure of tree size. Among these tall individuals, however, estimated axial fraction decreased with tree height ($R^2 = 0.95$). The tallest living tree (116 m) had only 4% of its total leaf area borne on axial shoots. Because of its low proportion of axial leaves, this individual had potential to absorb only $\sim 30 \text{ kg H}_2\text{O h}^{-1}$ during whole-crown leaf-wetting events despite having 5193 m^2 of projected leaf area (Table 4). Axial leaf area fraction decreased with height

in forests north of 40° latitude but increased with height in forests south of 38° latitude. *Sequoia* trees in the southernmost location (LH) had a greater whole-tree axial leaf area percent ($7.4 \pm 0.4\%$) than did trees growing in northern forests ($5.6 \pm 0.3\%$; Tables 1,3,4; Figure 4).

Initial surface permeability

Both peripheral and axial leaves were capable of foliar uptake at all crown positions, but initial surface permeability (maximum uptake) as derived from sample-specific flux curves, varied among sample-clusters. Axial-shoot permeability ($\bar{X} = 23.8 \text{ g H}_2\text{O m}^{-2}$) at estimated pre-dawn Ψ was significantly greater than the initial permeability to water seen in peripheral shoots ($\bar{X} = 7.1 \text{ g H}_2\text{O m}^{-2}$; Table 2). Initial permeability in peripheral shoots increased nonlinearly with start water potential (the initial Ψ gradient, assuming external droplet $\Psi = 0$), which was always very close to expected pre-dawn Ψ values estimated from sample height ($R^2 = 0.85$; Table 3, Figure 3C). In contrast, initial permeability ($\text{g H}_2\text{O m}^{-2}$) in axial shoots was unrelated to shoot Ψ when fogging began ($R^2 < 0.1$), though in multi-branch data, uptake ($\text{g H}_2\text{O m}^{-2} \cdot \text{min}^{-1}$; see Table 2) was related to Ψ in both shoot types (Table 3) and used for estimating whole-tree absorption capacity.

Structural equation models (SEMs)

We were able to fit a SEM describing initial surface permeability to water (maximum uptake) in peripheral shoots with a $R^2 = 0.955$ and a comparative fit index (CFI) of 0.952 (χ^2 of 6.013, $df = 4$, $P = 0.198$; Figure 3A). Surface resistance was caused by the collective effects of abaxial stomatal density, abaxial stomatal guard cell length per area, and abaxial surface wax coverage (Figure 3A). The effects of the initial Ψ gradient ($\Delta\Psi$) on uptake were ~30% greater than the effects of surface resistance. Because leaf traits can vary in association with height, we examined the importance of shared causality between traits and $\Delta\Psi$, which was height based, by removing $\Delta\Psi$ from the model and adding height as a predictor of all three traits and initial permeability. The resulting SEM had similar parameter estimates, with an $R^2 = 0.938$, a very low χ^2 of 0.034 ($df = 2$, $P = 0.983$), and a CFI of 1. However, despite the improved fit when height was used in place of $\Delta\Psi$, comparison of AIC_c scores indicated that the model with height was half as likely as the SEM with $\Delta\Psi$. We interpret the low likelihood of the model with height to mean that even though our final model (shown in Figure 3A) misses some of the variation in traits caused by factors associated with height, it is generally correct in elucidating the causes of surface resistance and uptake variation.

We were unable to identify a SEM of initial surface permeability (maximum uptake) in axial shoots or axial and peripheral shoots combined. A key leaf trait in both

peripheral and axial models, and the trait having the greatest univariate correlation with initial permeability, was the covering fraction of waxes on the abaxial surface (Figure 3B). All three traits in the SEM model were from the abaxial leaf surface, and no adaxial traits had strong univariate correlations with initial surface permeability.

DISCUSSION

Sequoia meets the contradictory challenges of wet and dry environments by allocating photosynthetic and water absorptive functions to two distinct and structurally specialized shoot types (Figure 1), absorbing up to 48 kg H₂O in the first hour of estimated foliar uptake, when we scale up to the whole crown (Table 4). Peripheral leaves (Figure 1) absorb less water than leaves of co-occurring conifers (Kerhoulas et al., 2020), but a waxy coating and densely packed stomata with wax plugs (Figures 2A, 3B) may support photosynthesis during extended wet periods at the price of increased surface resistance to water uptake (Figure 3). Axial leaves have more than three times the maximum uptake of peripheral leaves, allowing for more rapid foliar water absorption along the high-value woody axis that supports clusters of peripheral shoots. Axial leaves themselves may be largely nonphotosynthetic and have potential maintenance costs. Substantial foliar uptake—in the key woody support structures of all photosynthetic leaves—could permit embolism repair and vascular recharging, aligning with an ecological strategy of longevity where stress tolerance in vulnerable distal organs protects the tree.

Foliar water uptake in peripheral shoots behaves according to the expectations of Ohm's Law (Figure 3A), suggesting that is a physical process dependent on $\Delta\Psi$ as the driving force without the involvement of other processes that lower resistance over time (Figure 3A, C). Three leaf traits collectively cause surface resistance, and when controlling for $\Delta\Psi$, they explain 96% of the variation in the initial permeability of peripheral shoots to water. These traits—coverage of visible surface waxes, stomatal density, and guard cell length per leaf area—all respond to environmental signals (Baker, 1974; Hadley and Smith, 1989; Ashton and Berlyn et al., 1992; Gonzales and Ayerbe, 2010; Hronková et al., 2015; Salgado-Negret et al., 2015; Chin and Sillett, 2019). Environmental responsiveness of surface resistance could make uptake capacity subject to regional conditions, as in the fern *Polystichum munitum* (Limm and Dawson, 2010). Wax coverage in particular varies among samples and is the only trait we found to predict uptake in peripheral and axial shoots combined ($R^2 = 0.64$) better than within shoot type, suggesting that this may be a focal trait for future investigation of regional differences. The pathway water takes when entering *Sequoia* leaves is still unknown; wax coverage and stomatal density most strongly increase hydraulic resistance, suggesting that water crosses the cuticle, yet larger stomatal size modestly lowers resistance, indicating that some water may enter that way (Figure 3A).

In angiosperms, two-thirds of fog uptake enters leaves as vapor diffusing through stomata with the rest crossing the cuticle (Guzmán-Delgado et al., 2021); however, further work is needed to explore uptake pathways in conifers. Peripheral leaves with especially low visible wax coverage do not have uptake rates as high as axial shoots with comparable wax levels (Figure 3B), suggesting that other traits are influential. Interestingly, maximum axial-shoot uptake is uncorrelated with $\Delta\Psi$ ($R^2 < 0.00001$), implying that other passive or active mechanisms may impact the initial surface permeability to water. Uptake variation may be related to many factors not explored here, including a drop in surface resistance with increasing hydration of cuticular waxes, multiple physiological or physical factors that vary with leaf hydration, increases in internal capacity to transport water related to change in cell volume, or upregulation of aquaporins that actively increase water transport (Ohrui et al., 2007; Laur and Hacke, 2014). In addition, the abundance of epiphyllic organisms on the sheltered surface of decurrent axial leaves may enhance uptake capacity (Figure 2B; Holder, 2011). Axial shoots seem to provide an environment more conducive to epiphyllic growth, so it would be interesting to know whether axial leaves are less toxic and promote a symbiotic association.

Axial shoots do not appear to photosynthesize enough to contribute sugars to the tree, so costs of their construction and maintenance come at the expense of producing additional peripheral leaf area (Figure 4). Based on phloem anatomy and low stomatal density, our measurements of negligible axial-shoot photosynthetic rates in sun leaves on short trees are likely to apply to tall trees. However, even if axial shoots do make a sugar contribution in situ, it is unlikely that they match the photosynthetic rates of peripheral shoots under any conditions. If, instead of leaf retention, the green axial shoots were converted to bark, that same surface area would absorb ~2% of the water that axial leaves can contribute (Earles et al., 2016), a considerable hydraulic cost. It appears that something about axial leaves being green, whether lack of surface suberization, the presence of living parenchyma, or other factors, promotes uptake. Outsized investment in transfusion tissue area in axial leaves likely only serves a protective function while the leaf lives. Fractional investment in axial shoot area decreases with height in northern forests, but the southernmost forest we studied shows the opposite trend—concentrating axial leaves in the treetops (Figure 4). Treetop peripheral shoots may have the greatest potential for photosynthetic contribution based on access to light, so the construction of axial shoots presumably has a higher trade-off cost per area in southern forests where trees have a higher treetop axial fraction than in northern forests (Figure 4). Treetop axial leaves may be a necessity in relatively dry forests where summertime leaf wetting events are less frequent, of shorter duration, and trees are likely to be operating closer to their hydraulic limits (PRISM Climate Group, 2020; Table 1, Figure 4). Distance from the dew

point (difference between average minimum temperature and condensation threshold) could be of particular importance in driving differences in axial-leaf investment among locations (Tables 1, 3, 4; Figure 4), because leaf-wetting due to condensation may more effectively reach the entire tree, compared to small quantities of precipitation, which may be intercepted by the upper crown.

The potential trade-off between axial and peripheral shoot area is not solely a reflection of the availability of light and aerial water. It is complicated by the fact that axial shoots provide support for clusters of peripheral shoots, and axial leaves are maintained as green for varying lengths of time. In treetops, light availability should promote fractional investment in peripheral shoot area (lower ratio of axial to peripheral shoot area). However, where precipitation is at a premium and dew point may be reached infrequently (i.e., southern and range-margin forests; Table 1, Figure 4), trees maintain a higher axial leaf area fraction. When predicted axial leaf area investment is considered for individual trees, both crown structure and geographic location have large potential impacts on axial contributions to foliar uptake (Figure 4). In our study trees, axial shoots are estimated to contribute an extra 14–28% to whole-crown foliar uptake (Table 4). Based on isotopic analysis of leaves (Burgess and Dawson, 2004), this is roughly 1–2% of whole-tree water use, though ground-level isotopic studies (Burgess and Dawson, 2004) suggest that 30% of summertime water comes from fog, so the contribution of axial shoots may be many times greater because fog events are not always heavy enough to provide soil drip, and rain water absorption was not considered. Uptake of water by thin-barked, leafless twigs may support additional localized recovery (Earles et al., 2016). However, surface area of brown twigs <1 cm diameter, many of which are axial shoots with dead leaves, is 20× less than total leaf surface area (Sillett et al., 2015). With a bark uptake rate <10% that of peripheral leaves (based on data of Earles et al., 2016), thin-barked twigs thus seem to contribute a trivial fraction of total uptake capacity, even when their surface area is considered on a whole-crown level. Predicted patterns of axial shoot investment may lead to a larger water-uptake benefit per photosynthetic cost in northern forests, where axial shoot fraction is greatest in the shady lower crown, and more water uptake per total leaf area in dry southern forests, due to their greater whole-crown axial-shoot fraction (Table 4). Dimorphic division of labor promotes the longevity of shoot clusters by supporting dry-season survival and promoting carbon acquisition all year. Balancing axial and peripheral leaf areas allows *Sequoia* to protect key structures during dry summers through axial-shoot foliar water uptake, while freeing peripheral leaves to deploy surface traits that may help them avoid excessive water accumulation over stomata during prolonged wet periods (Smith and McClean, 1989; Hanba et al., 2004; Ambrose et al., 2010; Gerlein-Safidi et al., 2018). A longevity-focused life history requires the ability to recover from infrequent, but potentially severe water stress events and to avoid accumulation of minor damage. In the relatively dry forests of the southern range, the

need for hydraulic recovery may force prioritization of foliar water uptake through investment in treetop axial-shoot area characterized by marginal net photosynthesis (Figure 4). Surface hydraulic resistance is an underlying physical property caused by visible traits (Figure 3A, B), and it is these microscale features of leaves that respond to environmental signals, vary within and among trees (Rosado et al., 2010; Binks et al., 2019; Chin and Sillett, 2019), and likely drive regional variation in uptake capacity. Regional uptake differences may have large-scale impacts on forest hydrology and climate sensitivity (Holder, 2007b; Konrad et al., 2012; Shreel and Steppe, 2020), and it would be worthwhile to explore resistance-causing traits across tree geographic ranges in the future.

CONCLUSIONS

Axial shoots of *Sequoia* appear to be specialists in foliar water uptake, contrasting in both structure and function to abundant peripheral shoots, which appear to be responsible for nearly all photosynthesis. Rapid water absorption and abundant transfusion tissue in axial shoots may act together to secure the longevity of woody axes responsible for supporting productive peripheral shoots during California's long dry season. Axial shoot uptake may reduce the summertime accumulation of hydraulic damage, thereby protecting larger structures from loss and supporting tree survival during drought events. Our results suggest that leaf surface area in southern forests absorbs 10% more water per hour than in northern forests due to differences in axial shoot distribution (Figure 4). A suite of traits causes hydraulic resistance at the leaf surface, collectively influencing permeability to water. We thus suspect that climatic signals induce trait variation causing even larger geographic differences in the ways *Sequoia* crowns intercept and interact with precipitation. Broadleaved trees in seasonally wet forests can separate foliar uptake and gas exchange by having an absorptive adaxial surface as well as a water-resistant abaxial surface (Smith and McClean, 1989; Holder, 2007a; Eller et al., 2013; Fernandez et al., 2014). In conifers, limits to leaf width and shape imposed by a single vein (Zwieniecki et al., 2004) may make it harder for the abaxial surface of their needle-like leaves to remain dry if water accumulates on the adaxial surface to allow foliar uptake (Limm and Dawson 2010; Rosado et al., 2010; Fernández et al., 2014). Shoot dimorphism solves this problem and potentially allows *Sequoia* the flexibility to fine-tune investments in uptake capacity and photosynthesis across vertical and latitudinal gradients, supporting both growth and longevity.

AUTHOR CONTRIBUTIONS

A.R.O.C., P.G.D., and M.A.Z. designed the study; A.R.O.C., P.G.D., S.C.S., J.O., Z.J.M., and M.R. conducted the study; A.R.O.C. and M.A.Z. analyzed the uptake and trait data; S.C.S., L.P.K., and R.D.K. provided additional data and assisted in their interpretation and analysis in the context of

the present study. A.R.O.C. wrote the first draft of the manuscript, which was then completed with contributions and editorial input from all the other authors.

ACKNOWLEDGMENTS

The authors thank B. Chin for assistance with the experiment, A. McElrone for comments on the manuscript, M. Gilbert for helpful discussion, and J. Jernstedt for discussion of heteroblasty and use of her histology lab. We also thank the anonymous reviewers for their particularly helpful and detailed feedback. A.R.O.C. was supported by a Graduate Research Fellowship from NSF; P.G.-D. was supported by a Katherine Esau Fellowship from UC Davis. Open access funding provided by Eidgenössische Technische Hochschule Zurich.

DATA AVAILABILITY STATEMENT

Supporting data are publicly available online from ResearchGate at https://www.researchgate.net/publication/359005725_Data_for_Chin_et_al_2022_Shoot_dimorphism_paper (<https://doi.org/10.13140/RG.2.2.21254.24646>).

ORCID

Alana R. O. Chin  <http://orcid.org/0000-0002-3862-9563>

REFERENCES

- Ambrose, A. R., S. C. Sillett, G. W. Koch, R. Van Pelt, M. E. Antoine, and T. E. Dawson. 2010. Effects of height on treetop transpiration and stomatal conductance in coast redwood (*Sequoia sempervirens*). *Tree Physiology* 30: 1260–1272.
- Aparecido, L. M., G. R. Miller, A. T. Cahill, and G. W. Moore. 2017. Leaf surface traits and water storage retention affect photosynthetic responses to leaf surface wetness among wet tropical forest and semiarid savanna plants. *Tree Physiology* 37: 1285–1300.
- Ashton, P. M. S., and G. P. Berlyn. 1992. Leaf adaptations of some *Shorea* species to sun and shade. *New Phytologist* 121: 587–596.
- Baker, E. A. 1974. The influence of environment on leaf wax development in *Brassica oleracea* var. *gemmifera*. *New Phytologist* 73: 955–966.
- Berry, Z. C., and G. R. Goldsmith. 2020. Diffuse light and wetting differentially affect tropical tree leaf photosynthesis. *New Phytologist* 225: 143–153.
- Binks, O., M. Mencuccini, L. Rowland, A. C. da Costa, C. J. R. de Carvalho, P. Bittencourt, C. Eller, et al. 2019. Foliar water uptake in Amazonian trees: evidence and consequences. *Global Change Biology* 25: 2678–2690.
- Blonder, B. 2018. hypervolume: High dimensional geometry and set operations using kernel density estimation, support vector machines, and convex hulls. Website: <https://cran.r-project.org/package=hypervolume>
- Breshears, D. D., N. G. McDowell, K. L. Goddard, K. E. Dayem, S. N. Martens, C. W. Meyer, and K. M. Brown. 2008. Foliar absorption of intercepted rainfall improves woody plant water status most during drought. *Ecology* 89: 41–47.
- Burgess, S. S. O., and T. E. Dawson. 2004. The contribution of fog to the water relations of *Sequoia sempervirens* (D. Don): foliar uptake and prevention of dehydration. *Plant, Cell and Environment* 27: 1023–1034.
- Chin, A. R., and S. C. Sillett. 2016. Phenotypic plasticity of leaves enhances water-stress tolerance and promotes hydraulic conductivity in a tall conifer. *American Journal of Botany* 103: 796–807.
- Chin, A. R., and S. C. Sillett. 2019. Within-crown plasticity in leaf traits among the tallest conifers. *American Journal of Botany* 106: 174–186.

- Clark, J. W., and T. C. Scheffer. 1983. Natural decay resistance of the heartwood of coast redwood *Sequoia sempervirens* (D. Don) Endl. *Forest Products Journal* 33: 15–20.
- Davies, N. T., H. F. Wu, and C. M. Altaner. 2014. The chemistry and bioactivity of various heartwood extracts from redwood (*Sequoia sempervirens*) against two species of fungi. *New Zealand Journal of Forestry Science* 44: 17.
- Dawson, T. E., and G. R. Goldsmith. 2018. The value of wet leaves. *New Phytologist* 219: 1156–1169.
- Earles, M. J., O. Sperling, L. C. Silva, A. J. McElrone, C. R. Brodersen, M. P. North, and M. A. Zwieniecki. 2016. Bark water uptake promotes localized hydraulic recovery in coastal redwood crown. *Plant, Cell and Environment* 39: 320–328.
- Eller, C. B., A. L. Lima, and R. S. Oliveira. 2013. Foliar uptake of fog water and transport belowground alleviates drought effects in the cloud forest tree species. *Drimys brasiliensis* (Winteraceae). *New Phytologist* 199: 151–162.
- Emery, N. C. 2016. Foliar uptake of fog in coastal California shrub species. *Oecologia* 182: 731–742.
- Fernández, V., D. Sancho-Knapik, P. Guzmán, J. J. Peguero-Pina, L. Gil, G. Karabourniotis, M. Khayet, et al. 2014. Wettability, polarity, and water absorption of holm oak leaves: effect of leaf side and age. *Plant Physiology* 166: 168–180.
- Fritz, E. 1931. The role of fire in the redwood region. *Journal of Forestry* 29: 939–950.
- Gerlein-Safdi, C., M. C. Koochafkan, M. Chung, F. E. Rockwell, S. Thompson, and K. K. Caylor. 2018. Dew deposition suppresses transpiration and carbon uptake in leaves. *Agricultural and Forest Meteorology* 259: 305–316.
- Gotsch, S. G., N. Nadkarni, A. Darby, A. Glunk, M. Dix, K. Davidson, and T. E. Dawson. 2015. Life in the treetops: ecophysiological strategies of canopy epiphytes in a tropical montane cloud forest. *Ecological Monographs* 85: 393–412.
- Grace, J. B. 2006. Structural equation modeling and natural systems. Cambridge University Press, Cambridge, UK.
- Guzmán-Delgado, P., Laca, and M. A. Zwieniecki. 2021. Unravelling foliar water uptake pathways: the contribution of stomata and the cuticle. *Plant, Cell & Environment* 44: 1728–1740.
- Guzmán-Delgado, P., J. Mason Earles, and M. A. Zwieniecki. 2018. Insight into the physiological role of water absorption via the leaf surface from a rehydration kinetics perspective. *Plant, Cell and Environment* 41: 1886–1894.
- Hadley, J. L. and W. K. Smith. 1989. Wind erosion of leaf surface wax in alpine timberline conifers. *Arctic and Alpine Research* 21: 392–398.
- Hanba, Y. T., A. Moriya, and K. Kimura. 2004. Effect of leaf surface wetness and wettability on photosynthesis in bean and pea. *Plant, Cell and Environment* 27: 413–421.
- Holder, C. D. 2007a. Leaf water repellency as an adaptation to tropical montane cloud forest environments. *Biotropica* 39: 767–770.
- Holder, C. D. 2007b. Leaf water repellency of species in Guatemala and Colorado (USA) and its significance to forest hydrology studies. *Journal of Hydrology* 336: 147–154.
- Holder, C. D. 2011. The relationship between leaf water repellency and leaf traits in three distinct biogeographical regions. *Plant Ecology* 212: 1913.
- Hronková, M., D. Wiesnerová, M. Šimková, P. Skúpa, W. Dewitte, M. Vráblová, E. Vráblová, E. Zažimalová, E., and J. Šantrůček. 2015. Light-induced STOMAGEN-mediated stomatal development in Arabidopsis leaves. *Journal of Experimental Botany* 66: 4621–4630.
- Ishibashi, M., and I. Terashima. 1995. Effects of continuous leaf wetness on photosynthesis: adverse aspects of rainfall. *Plant, Cell and Environment* 18: 431–438.
- Jones, C. S. 1999. An essay on juvenility, phase change, and heteroblasty in seed plants. *International Journal of Plant Sciences* 160: S105–S111.
- Kerhoulas, L. P., A. S. Weisgrau, E. C. Hoefl, and N. J. Kerhoulas. 2020. Vertical gradients in foliar physiology of tall *Picea sitchensis* trees. *Tree Physiology* 40: 321–332.
- Konrad, W., M. Ebner, C. Traiser, and A. Roth-Nebelsick. 2012. Leaf surface wettability and implications for drop shedding and evaporation from forest canopies. *Pure and Applied Geophysics* 169: 835–845.
- Kramer, R. D., S. C. Sillett, and A. L. Carroll. 2014. Structural development of redwood branches and its effects on wood growth. *Tree Physiology* 34: 314–330.
- Laur, J., and U. G. Hacke. 2014. Exploring *Picea glauca* aquaporins in the context of needle water uptake and xylem refilling. *New Phytologist* 203: 388–400.
- Lawson, T., and J. Matthews. 2020. Guard cell metabolism and stomatal function. *Annual Review of Plant Biology* 71: 273–302.
- Limm, E. B., and T. E. Dawson. 2010. *Polystichum munitum* (Dryopteridaceae) varies geographically in its capacity to absorb fog water by foliar uptake within the redwood forest ecosystem. *American Journal of Botany* 97: 1121–1128.
- Limm, E. B., K. A. Simonin, A. G. Bothman, and T. E. Dawson. 2009. Foliar water uptake: a common water acquisition strategy for plants of the redwood forest. *Oecologia* 161: 449–459.
- Neinhuis, C., and W. Barthlott. 1997. Characterization and distribution of water-repellent, self-cleaning plant surfaces. *Annals of Botany* 79: 667–677.
- Ohrui, T., H. Nobira, Y. Sakata, T. Taji, C. Yamamoto, K. Nishida, T. Yamakawa, et al. 2007. Foliar trichome- and aquaporin-aided water uptake in a drought-resistant epiphyte *Tillandsia ionantha* Planchon. *Planta* 227: 47–56.
- Oldham, A. R., S. C. Sillett, A. M. Tomescu, and G. W. Koch. 2010. The hydrostatic gradient, not light availability, drives height-related variation in *Sequoia sempervirens* (Cupressaceae) leaf anatomy. *American Journal of Botany* 97: 1087–1097.
- PRISM Climate Group. 2020. PRISM Data Explorer: Norm81m dataset. PRISM Climate Group, Northwest Alliance for Computation Science and Engineering, Oregon State University, Corvallis, OR, USA. Available at <https://prism.oregonstate.edu/>
- Rosado, B. H. P., R. S. Oliveira, and M. P. M. Aidar. 2010. Is leaf water repellency related to vapor pressure deficit and crown exposure in tropical forests? *Acta Oecologica* 36: 645–649.
- Rosseel, Y. 2012. lavaan: an R package for structural equation modeling. *Journal of Statistical Software* 48: 1–36.
- Rundel, P. W. 1982. Water uptake by organs other than roots. In O. L. Lange, P. S. Nobel, C. B. Osmond, and H. Ziegler [eds.], *Physiological plant ecology II*, 111–134. Springer, Berlin, Germany.
- Salgado-Negret, B., R. Canessa, F. Valladares, J. J. Armesto, and F. Pérez. 2015. Functional traits variation explains the distribution of *Aextoxiccon punctatum* (Aextoxicaceae) in pronounced moisture gradients within fog-dependent forest fragments. *Frontiers in Plant Science* 6: 511.
- Schreel, J. D., and K. Steppe. 2020. Foliar water uptake in trees: negligible or necessary? *Trends in Plant Science* 25: 590–603.
- Schreel, J. D., J. S. von der Crone, O. Kangur, and K. Steppe. 2019. Influence of drought on foliar water uptake capacity of temperate tree species. *Forests* 10: 562.
- Sillett, S. C., M. E. Antoine, J. Campbell-Spickler, A. L. Carroll, E. J. Coonen, R. D. Kramer, and K. H. Scarla. 2018. Manipulating tree crown structure to promote old-growth characteristics in second-growth redwood forest canopies. *Forest Ecology and Management* 417: 77–89.
- Sillett, S. C., R. D. Kramer, R. Van Pelt, A. L. Carroll, J. Campbell-Spickler, and M. E. Antoine. 2021. Comparative development of the four tallest conifer species. *Forest Ecology and Management* 480: 118688.
- Sillett, S. C., R. Van Pelt, A. L. Carroll, J. Campbell-Spickler, and M. E. Antoine. 2020. Aboveground biomass dynamics and growth efficiency of *Sequoia sempervirens* forests. *Forest Ecology and Management* 458: 117740.
- Sillett, S. C., R. Van Pelt, A. L. Carroll, R. D. Kramer, A. R. Ambrose, and D. A. Trask. 2015. How do tree structure and old age affect growth potential of California redwoods? *Ecological Monographs* 85: 181–212.
- Sillett, S. C., R. Van Pelt, G. W. Koch, A. R. Ambrose, A. L. Carroll, M. E. Antoine, and B. M. Mifsud. 2010. Increasing wood production through old age in tall trees. *Forest Ecology and Management* 259: 976–994.

- Smith, W. K., and T. M. McClean. 1989. Adaptive relationship between leaf water repellency, stomatal distribution, and gas exchange. *American Journal of Botany* 76: 465–469.
- Steppe, K., M. W. Vandegehuchte, B. A. Van de Wal, P. Hoste, A. Guyot, C. E. Lovelock, and D. A. Lockington. 2018. Direct uptake of canopy rainwater causes turgor-driven growth spurts in the mangrove *Avicennia marina*. *Tree Physiology* 38: 979–991.
- Van Pelt, R., S. C. Sillett, W. A. Kruse, J. A. Freund, and R. D. Kramer. 2016. Emergent crowns and light-use complementarity lead to global maximum biomass and leaf area in *Sequoia sempervirens* forests. *Forest Ecology and Management* 375: 279–308.
- Yates, D. J., and L. B. Hutley. 1995. Foliar uptake of water by wet leaves of *Sloanea woollsi*, an Australian subtropical rainforest tree. *Australian Journal of Botany* 43: 157–167.
- Zimmermann, M. H. 1983. Xylem structure and the ascent of sap. Springer-Verlag, Berlin, Germany.
- Zwieniecki, M. A., C. K. Boyce, and N. M. Holbrook. 2004. Functional design space of single-veined leaves: role of tissue hydraulic properties in constraining leaf size and shape. *Annals of Botany* 94: 507–513.

How to cite this article: Chin, A. R. O., P. Guzmán-Delgado, S. C. Sillett, J. Orozco, R. D. Kramer, L. P. Kerhoulas, Z. J. Moore, M. Reed, and M. A. Zwieniecki. 2022. Shoot dimorphism enables *Sequoia sempervirens* to separate requirements for foliar water uptake and photosynthesis. *American Journal of Botany* 109(4): 564–579. <https://doi.org/10.1002/ajb2.1841>